Molecular Biology of the Cell
Vol. 14, 2508–2519, June 2003

α-Smooth Muscle Actin Is Crucial for Focal Adhesion Maturation in Myofibroblasts[V]

Boris Hinz,*† Vera Dugina,‡ Christoph Ballestrem,§ Bernhard Wehrle-Haller,* Christine Chaponnier*

*Department of Pathology, Centre Medical Universitaire, University of Geneva, 1211 Geneva 4, Switzerland; ‡Moscow State University, 119899 Moscow, Russia; and §Department of Molecular Cell Biology, The Weizmann Institute of Science, 76100 Rehovot, Israel

Submitted November 13, 2002; Revised December 23, 2002; Accepted February 5, 2003
Monitoring Editor: Paul T. Matsudaira

Cultured myofibroblasts are characterized by stress fibers, containing α-smooth muscle actin (α-SMA) and by supermature focal adhesions (FAs), which are larger than FAs of α-SMA–negative fibroblasts. We have investigated the role of α-SMA for myofibroblast adhesion and FA maturation. Inverted centrifugation reveals two phases of initial myofibroblast attachment: during the first 2 h of plating microfilament bundles contain essentially cytoplasmic actin and myofibroblast adhesion is similar to that of α-SMA–negative fibroblasts. Then, myofibroblasts incorporate α-SMA in stress fibers, develop mature FAs and their adhesion capacity is significantly increased. When α-SMA expression is induced in 5 d culture by TGFβ or low serum levels, fibroblast adhesion is further increased correlating with a "supermaturation" of FAs. Treatment of myofibroblasts with α-SMA fusion peptide (SMA-FP), which inhibits α-SMA–mediated contractile activity, reduces their adhesion to the level of α-SMA negative fibroblasts. With the use of flexible micropatterned substrates and EGFP-constructs we show that SMA-FP application leads to a decrease of myofibroblast contraction, shortly followed by disassembly of paxillin- and β3 integrin-containing FAs; α5 integrin distribution is not affected. FRAP of β3 integrin-EGFP demonstrates an increase of FA protein turnover following SMA-FP treatment. We conclude that the formation and stability of supermature FAs depends on a high α-SMA–mediated contractile activity of myofibroblast stress fibers.

INTRODUCTION

Myofibroblasts are specialized fibroblastic cells that appear during wound healing and in a variety of fibrocontractive diseases where they exert a significant contractile activity (for a review see Serini and Gabbiani, 1999); they are characterized by well-developed microfilament bundles (Gabbiani *et al.,* 1971), which are analogous to stress fibers of fibroblasts in culture. In contrast, resident tissue fibroblasts do not exhibit such a contractile apparatus (for a review see Tomasek *et al.,* 2002). On stimulation with TGFβ (Desmoulière *et al.,* 1993; Rønnov-Jessen and Petersen, 1993) myofibroblasts express de novo α-smooth muscle actin (α-SMA; Skalli *et al.,* 1986) and form specialized adhesion structures with the ECM that are called fibronexus in vivo (Singer *et al.,* 1984) or "supermature" focal adhesions (FAs) in vitro (Dugina *et al.,* 2001).

Cultured fibroblasts are mechanically coupled to and communicate with the ECM through a range of different adhesion sites that all contain transmembrane receptors belonging to the integrin family and cytoplasmic actin (Geiger *et al.,* 2001). The multiplicity of activities that are asked from these adhesions such as signaling, ECM reorganization, cell migration and physical anchorage is reflected in their complex and diverse molecular composition (for reviews see Hynes, 1999; Calderwood *et al.,* 2000; Adams, 2001; Geiger *et al.,* 2001). They can be classified into focal complexes, classical FAs, and fibrillar adhesions using as criteria their size, intracellular localization, morphology, and molecular composition (Zamir *et al.,* 1999). Recently, mechanical stress has been identified as one of the most important factors defining the fate of these different adhesion types (for a review see Geiger and Bershadsky, 2001). Focal complexes (Nobes and

Article published online ahead of print. Mol. Biol. Cell 10.1091/mbc.E02–11–0729. Article and publication date are available at www.molbiolcell.org/cgi/doi/10.1091/mbc.E02–11–0729.

[V] Online version of this article contains video material. Online version is available at www.molbiolcell.org.

† Corresponding author. E-mail address: boris.hinz@epfl.ch.

Abbreviations used: α-SMA, α-smooth muscle actin; FA, focal adhesion; FN, fibronectin; FP, fusion peptide; LF, lung fibroblast; PFA, paraformaldehyde; SKA, skeletal actin; SM, smooth muscle; TGFβ-RII, TGFβ soluble receptor type II; Triton X-100, TX-100.

Hall, 1995; Clark *et al.*, 1998) originate as dot-like structures of ~1 μm^2 and are generally described to form in a tension-independent manner, although some reports demonstrated their dissociation after inhibition of actomyosin-mediated contractile activity (Rottner *et al.*, 1999). Focal complexes mature into FAs upon increase of intracellular (Chrzanowska Wodnicka and Burridge, 1996) and/or extracellular tension (Riveline *et al.*, 2001). These classical FAs are ~2–5-μm long and typically contain $\alpha v\beta 3$ integrin, vinculin, paxillin, and talin (Geiger *et al.*, 2001). Concomitant with fibroblast differentiation into myofibroblasts, mature FAs increase their length to 6–30 μm and transform into supermature FAs, which differ from classical FAs by expressing significant levels of tensin (Dugina *et al.*, 2001). Tensin is often used as a marker for fibrillar adhesions, which in contrast to supermature and classical FAs contain only traces of paxillin, no vinculin and $\beta 3$ integrin but $\alpha 5\beta 1$ integrin; they function as fibronectin (FN)-organizing organelles and are insensitive to inhibition of intracellular contractile activity (Zamir *et al.*, 1999); moreover, they are not associated with stress fibers but with thin actin fibers (Katz *et al.*, 2000).

Recently, it has been demonstrated that the occurrence of supermature FAs is closely related to the expression of α-SMA (Dugina *et al.*, 2001). Expression of α-SMA had been shown to increase fibroblast contractile activity (Arora and McCulloch, 1994; Hinz *et al.*, 2001a) and to decrease fibroblast motility (Rønnov Jessen and Jensen, 1996). Although the molecular composition of supermature FAs has been studied in detail, their function is not known, and it remains unclear whether their formation and maintenance depend on the expression of α-SMA in stress fibers. To address these questions, we analyzed the correlation between α-SMA expression in stress fibers, FA supermaturation, and cell adhesion strength in fibroblasts during spreading and in long-term culture. To test more specifically whether α-SMA–mediated contractile activity affects supermature FAs, we inhibited this action by means of the α-SMA fusion peptide (SMA-FP). SMA-FP contains the N-terminal sequence Ac-EEED of α-SMA, which is important for actin polymerization (Chaponnier *et al.*, 1995) and myofibroblast contractile activity in vivo and in vitro (Hinz *et al.*, 2002). Our results demonstrate that the expression level of α-SMA in stress fibers correlates with the degree of FA maturation and the strength of fibroblast adhesion. Inhibition of myofibroblast contractile activity by the SMA-FP leads to the disassembly of supermature FAs and decreases cell adhesion. We propose a model where expression of the contractile protein α-SMA increases the intracellular mechanical stress on FAs and thereby induces their supermaturation.

MATERIALS AND METHODS

Cell Culture

Rat lung (LF) and subcutaneous fibroblasts (SCF) were obtained and cultured as described previously (Hinz *et al.*, 2001a); REF-52 were cultured in DMEM (Life Technologies, Basel, Switzerland) containing 10% FCS. TGFβ1 (10 ng/ml, R&D Systems, Inc., Minneapolis, MN) and TGFβ-RII (250 ng/ml, gift of Biogen Inc., Cambridge, MA; Komesli *et al.*, 1998) were added for 5 d to the culture medium. FPs, consisting of a cell-penetrating vector (Derossi *et al.*, 1994) and the α-SMA N-terminal sequence AcEEED (SMA-FP) or the α-skeletal actin N-terminus AcDEDE (SKA-FP), respectively, were produced as described previously (Hinz *et al.*, 2002) and used in concentrations from 1 to 10 μg/ml.

Adhesion Assays

To avoid specific effects due to the substrate composition, we have coated all surfaces for 4 h with 20% FCS. FCS coating gave similar results on cell adhesion and contact morphology compared with a mixture of 10 μg/ml vitronectin and FN (Sigma, Buchs, CH) as tested in preliminary experiments. Immunofluorescence confirmed the availability of both ECM proteins in excess on FCS-coated surfaces. To test their adhesion capacity during spreading, fibroblasts were trypsinized and seeded on 96-well plates (5000 cells/well) that had been coated. FPs (5 μg/ml) were added 30 min after plating cells. All experiments using FPs were performed in serum-free F12 medium (Life Technologies) in order to reduce precipitation with soluble serum proteins (Hinz *et al.*, 2002). After 0.5–9 h the plate was inversely centrifuged for 10 min at 2000 rpm ($900 \times g$), and the amount of remaining cells was assessed by crystal violet staining (Wilkins *et al.*, 1991). In a preliminary experimental series, $900 \times g$ was determined to be the maximum force applicable without destroying strongly attaching cells; forces above this value lead to loss of the nucleus and cell breakage. To evaluate α-SMA filament bundle formation, cells were plated on six-well plates (50,000 cells/well) and fixed either directly or after inverted centrifugation, followed by α-SMA and F-actin immunostaining (see below).

To test fibroblast adhesion after long culture periods, REF-52 were pregrown for 5 d in F12 medium, containing 2, 5, 10, and 20% FCS, 2% FCS plus TGFβ-RII, and 10% FCS plus TGFβ and then seeded onto coated 96-well plates (5000 cells/well). After 2 d plating cells were briefly washed, treated with FPs (5 μg/ml) for 60 min, incubated with 0.02% EDTA/PBS plus FPs for another 60 min, and inversely centrifuged at 2000 rpm ($900 \times g$) for 10 min. Adhesion of FP-treated cells was normalized to untreated cells on the same plate. To detach fibroblasts after 2-d culture, it was crucial to unspecifically reduce integrin binding strength by chelating bivalent cations in the medium with EDTA; this step was not required in the case of early spreading fibroblasts (see above).

Flexible Polyacrylamide Substrates

Flexible polyacrylamide substrates with a thickness of 70 μm were produced on 35-mm round glass coverslips basically as described by Pelham and Wang (1997). First, we determined the optimal substrate stiffness to obtain α-SMA expression, FA supermaturation and detectable deformation by varying the BIS concentration. Gel stiffness was macroscopically determined as described (Pelham and Wang, 1997) and the calculated Young's modulus ranged from 4.8 N/m^2 at 0.025% BIS (flexible) to 38.2 N/m^2 at 0.15% BIS (stiff). All substrates were covalently coated with 0.1% poly-L-lysine solution (Sigma) using sulfo-SANPAH (Pelham and Wang, 1997) and post-coated with 20% FCS for 4 h. REF-52 were plated for 5 d, fixed, and stained for α-SMA, F-actin, and nuclei (see below); the average percentage of α-SMA–expressing cells was determined microscopically (20× objective) from five regions per substrate in three experiments.

To simultaneously visualize cell contractile activity and FAs, low compliant polyacrylamide gels (0.075% BIS, Young's modulus of 18.8 N/m^2) were provided with a micropattern using Si wafers as a mold (Balaban *et al.*, 2001). Si wafers (a kind gift of Dr. J.A. Hubbell, ETH Zurich, Switzerland) were produced by standard photolithography as previously described with a 5×5-μm surface pattern and a mold depth of 20 nm, as determined by atomic force microscopy (Michel *et al.*, 2002). Observation chambers were produced by gluing a silicone ring (i.d. 25 mm) onto the polyacrylamide containing coverslip.

Antibodies, Immunofluorescence, Confocal Microscopy, and FA Morphometry

Cells were permeabilized for 5 min with 0.2% Triton X-100 (TX-100) in 3% paraformaldehyde (PFA) and fixed with 3% PFA/PBS for 10 min. In the case of integrin detection this procedure was followed by 5-min treatment with methanol (−20°C). We used antibodies against paxillin (IgG1 mAb) and tensin (IgG2b mAb, Transduction Laboratories, Lexington, KY), β3 integrin (biotin-conjugated IgG hamAb 2C9.G2, PharMingen, Rockford, IL), α5β1 integrin (rbAb, a kind gift of V. Belkin, Hematological Scientific Center, Moscow, Russia; Dugina *et al.*, 2001), vinculin (hVin-1, IgG1 mAb, Sigma), α-SMA (αSM-1, IgG2a mAb; Skalli *et al.*, 1986), β-cytoplasmic actin (β74, rbAb; Yao *et al.*, 1995) and EGFP (rbAb and IgG1 mAb, Molecular Probes, Eugene, OR). As secondary antibodies we used TRITC- and FITC-conjugated goat anti-mouse subclasses IgG1 and IgG2a (Southern Biotechnology Associates Inc., Birmingham, AL), aminomethylcoumarin acetate-conjugated goat anti-rabbit antibodies (AMCA, Jackson ImmunoResearch Laboratories, West Grove, PA), Alexa 488-, Alexa 568-, and Cy5-conjugated IgG antibody, and goat anti-rabbit antibodies (Molecular Probes). Biotinylated anti-β3 integrin was probed with Streptavidin-Alexa 488 and F-actin with Phalloidin-Alexa 488 (Molecular Probes). Images were acquired using an oil immersion objective on an Axiophot microscope (Plan-Neofluar 63×/1.3 Ph3, Carl Zeiss Inc., Jena, Germany) equipped with a digital color camera and corresponding software (Axiocam, Zeiss) or with a confocal microscope (LSM510, Zeiss) with similar optics at 1.5× zoom. Confocal images were reconstructed from three optical sections with a depth of 0.2 μm. Images were processed with the use of Adobe Photoshop. For morphometry of FAs, REF-52 were double-stained for vinculin and α-SMA and the area of vinculin-stained FAs was measured on confocal images using KS400 software (Zeiss) as described before (Dugina *et al.*, 2001); mean values were calculated from at least 10 cells (~1.500 FAs) from five independent experiments per condition.

EGFP Constructs

We transfected REF-52 with β3 integrin-EGFP (Ballestrem *et al.*, 2001), full-length Paxillin-EGFP (a kind gift of Dr. B. Geiger, The Weizmann Institute of Science, Israel, Zamir *et al.*, 2000), and α5 integrin-EGFP (a kind gift of Dr. A.F. Horwitz, University of Virginia, VA; Laukaitis *et al.*, 2001), using Fugen 6 (Roche, Reinach, Switzerland) according to the manufacturers' protocol. Populations were selected for stable expression in culture medium containing 2 mg/ml G418 (Life Technologies) and regularly batch-sorted for medium EGFP-expression using a FACS sorter (FACStar+, Becton Dickinson AG, Allschwil, Switzerland).

Time-Lapse, Video Microscopy, Intensity Measurements, and FRAP

For all live studies, cells were cultured for 5 d in DMEM/10% FCS (±TGFβ) on 20% FCS-coated observation chambers (see above) and recorded in serum-free medium; in preliminary experiments serum depletion showed no effect on FA dynamics during 4 h of recording. Cells were observed with an Axiovert 100 TV inverted microscope (Zeiss), equipped with a heating stage and CO_2 incubation chamber, standard EGFP filter set (Omega Optical Inc., Brattleboro, VT) and a digital CCD camera (C4742-95-10, Hamamatsu Photonics, Massy Cedex, France). Cells were recorded with Openlab 3.0.6 software (Improvision, Basel, CH) with frame intervals of 2.5 min for 30 min in control conditions and then treated with FPs (5 μg/ml) and observed for another 120 min. To quantify changes of protein density in FAs, the EGFP-fluorescence intensity in FAs and fibrillar adhesions was measured on every second (5 min) inverted 8-bit grayscale TIF-image using the eyedropper tool of Adobe Photoshop 5.5. In detail, the black proportion of a 3 × 3-pixel region over the contact was corrected for membrane fluorescence and related to the intensity obtained from the first frame. For each EGFP-construct, mean values were calculated from 5 to 10 cells and 20 FAs per cell on 24 consecutive frames (120 min).

For FRAP, cells were mounted on an inverted confocal microscope equipped with a heating stage and CO_2 incubation chamber (LSM510, Zeiss). FPs were added 1 h before recording at 1 μg/ml; at this low concentration the dissociation of FAs was retarded. Image sequences were recorded with open pinhole using a 63 × objective (Zeiss) and 1.5× zoom with 0.2% laser transmission power (λ = 488 nm). The EGFP fluorescence of 12 peripheral FAs per leading cell edge was bleached with 35% transmission (λ = 458/488/514 nm) with seven iterations lasting 1 s, respectively. Control bleaching experiments over entire cells demonstrated complete EGFP-inactivation and no FRAP due to newly synthesized EGFP within 3 h. FRAP was quantified (LSM510 image analysis software, Zeiss) after background subtraction by normalizing the fluorescence intensities of 12 bleached to those of 12 unbleached neighboring contacts per cell as previously described (Ballestrem *et al.*, 2001). Obtained values were related to the fluorescence intensity just after bleaching (fractional recovery), and mean values were calculated per cell (12 cells).

Cell Fractionation and Western Blot Analysis

To assess association of proteins with the TX-100–insoluble cytoskeleton, cytosolic proteins were extracted for 2 × 5 min with ice-cold extraction buffer (0.5% TX-100, 60 mM Pipes, 25 mM HEPES, 10 mM EGTA, 2 mM $MgCl_2$, 1 mM Na-orthovanadate, pH 6.9), supplemented with protease inhibitors (Complete-EDTA, Boehringer Mannheim, Mannheim, Germany) as described before (Dugina *et al.*, 2001). Remaining TX-100–insoluble cytoskeletal proteins were thoroughly scraped from the culture dish and suspended in the same volume of extraction buffer. These fractions and total cell lysates were run on 10% SDS-minigels (Bio-Rad Laboratories AG, Glattbrugg, Switzerland) and blotted, and proteins were probed with the same primary antibodies used for immunofluorescence. HRP-conjugated secondary antibodies goat anti-mouse IgG and goat anti-rabbit IgG (Jackson ImmunoResearch Laboratories) and streptavidin-HRP (DAKO, Glostrup, Denmark) were detected by ECL chemiluminescence (Amersham, Rahn AG, Zürich, Switzerland); bands were digitized with a scanner (Arcus II, Agfa, Köln, Germany), and the ratio between all band densities of one blot was calculated by computer software (ImageQuant V3.3, Molecular Dynamics, Sunnyvale, CA); correct loading was tested by probing vimentin expression (clone V9, DAKO).

Statistical Analysis

Mean values are presented ± SD and tested by a two-tailed heteroscedastic Student's *t* test. Differences were considered to be statistically significant at $p \leq 0.05$, indicated by an asterisk (*) and marked with a double-asterisk (**) for $p \leq 0.001$. We tested the linear correlation between cytoskeletal protein expression and fibroblast adhesion by calculating the square of the Pearson correlation product (r^2 value).

RESULTS

Filament Bundles of Early Spreading Myofibroblasts Contain Only Cytoplasmic Actin

To investigate the incorporation of α-SMA into filament bundles in relation with FA maturation, we stained spreading REF-52 for α-SMA, β-cytoplasmic actin, and various FA proteins. During the first 2 h of cell spreading, the lamellae of circularly shaped REF-52 contained small bundles of β-cytoplasmic actin (Figure 1A); α-SMA staining was diffuse throughout the cytoplasm (Figure 1B). Initial adhesion sites

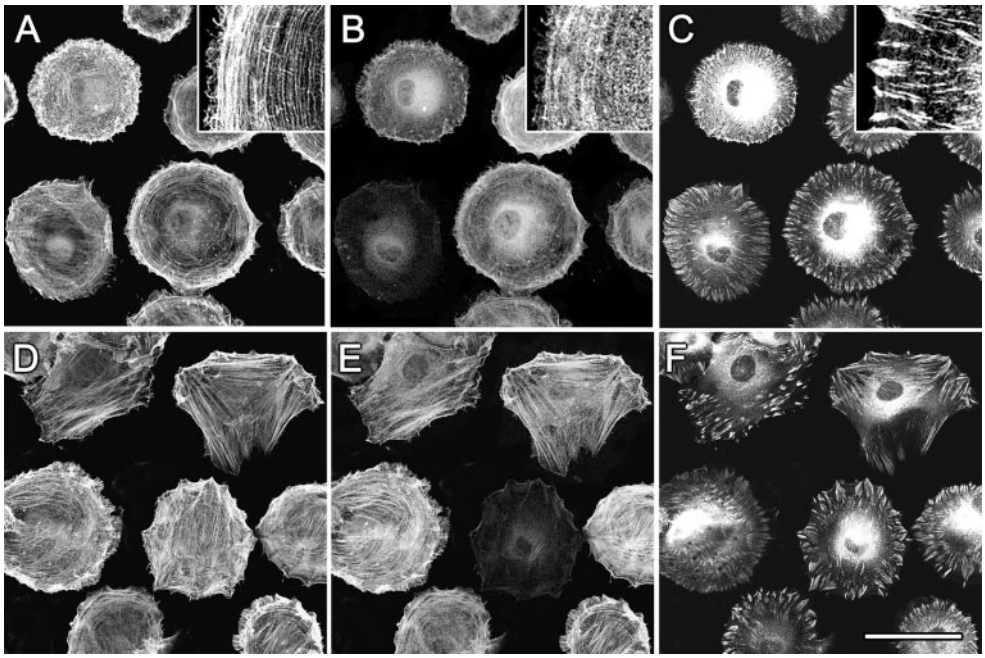

Figure 1. Filament bundles of early spreading myofibroblasts contain only β-cytoplasmic actin. REF-52 fibroblasts were trypsinized and plated for 2 h (A–C) and 3 h (D–F) and then fixed and triple-immunostained against β-cytoplasmic actin (A and D), α-SMA (B and E), and vinculin (C and F). Insets show at high magnification diffuse organization of α-SMA in the presence of β-cytoplasmic actin filament bundles. Incorporation of α-SMA into stress fibers starts 3 h after plating, correlating with FA maturation and cell polarization. Bar, 50 μm.

were arranged perpendicular to the cell edge and were positive for paxillin, β3-integrin (our unpublished results), and vinculin (Figure 1C). α-SMA started to appear in filament bundles 3 h after plating (Figure 1E), a time point that correlated with cell polarization and formation of first prominent stress fibers (Figure 1D). At that time cell polarization and formation of FAs out of initial adhesion sites was almost exclusively observed in association with α-SMA–positive stress fibers (Figure 1F); however, such cells exhibited similar spreading areas compared with cells without α-SMA–positive fibers. In α-SMA–negative fibroblasts, FAs appeared in relation to stress fibers starting 4 h after plating. Similar results were obtained using primary rat LF and SCF (our unpublished results). Densitometry of western blots performed with TX-100–soluble and –insoluble fractions of spreading myofibroblasts demonstrated that 1 h after of plating 55% of β cytoplasmic actin and 90% of vimentin were stabilized in the TX-100–insoluble cytoskeleton; these percentages did not change with time. In contrast, TX-100–insoluble α-SMA increased from 25% after 1 h to 70% after 3 h, correlating with the TX-100-insolubility of vinculin and paxillin (Figure 2B). Thus, formation of TX-100–insoluble β-cytoplasmic actin filament bundles clearly precedes incorporation of α-SMA into the cytoskeletal fraction.

During Spreading Fibroblast Adhesion Increases with the Formation of α-SMA Bundles

To test whether expression of α-SMA in stress fibers changes the adhesion strength of spreading myofibroblasts, we modulated α-SMA expression by TGFβ and its antagonist TGFβ-RII. In control conditions, 70 ± 5% REF-52 express α-SMA; this fraction was increased by TGFβ to 94 ± 6% and decreased by TGFβ-RII to 3%±2, which we defined as α-SMA negative (Figure 3A, inset). These different populations were then trypsinized, plated for 0.5–9 h, and inversely centrifuged, in order to select strongly adhering cells. Inverted centrifugation revealed only one phase of weak attachment in α-SMA–negative fibroblast populations (phase 1, Figure 3A, TGFβ-RII) but demonstrated a second phase of strong attachment in populations containing α-SMA–expressing cells (phase 2, control, TGFβ). Phase 1 correlated with β-cytoplasmic actin bundle formation, whereas phase 2 started 3 h after plating and correlated with α-SMA incorporation into stress fibers. To evaluate whether organization of α-SMA into fibers contributed to phase 2 of strong adhesion, we fixed and immunostained cells after normal spreading and after inverted centrifugation. In the usual control population, 19 ± 2% of fibroblasts incorporated α-SMA into filament bundles 3 h after plating. Centrifugation selected essentially fibroblasts with α-SMA filament bundles (78 ± 7%, Figure 3B). A similar selection of highly adhering α-SMA–positive fibroblasts was observed when we used primary fibroblast cultures with a constitutively low number of α-SMA–expressing cells, such as SCF (20%, our unpublished results) or LF, containing 70% α-SMA–positive cells in control conditions.

To further study the contribution of α-SMA expression to cell adhesion, we added the SMA-FP during spreading of REF-52. SMA-FP had no effect on α-SMA–negative REF-52 (Figure 3C) and did not influence adhesion of α-SMA–positive cells in phase 1 (Figure 3D); however, it completely inhibited adhesion in phase 2 (Figure 3D). The SKA-FP used as control was without effect in all conditions tested. These data suggest that the incorporation of α-SMA into stress fibers significantly improves FA maturation. Two populations of fibroblasts with different adhesion properties can be distinguished: strongly adhering α-SMA–positive fibroblasts and weakly adhering fibroblasts, expressing no or low levels of α-SMA.

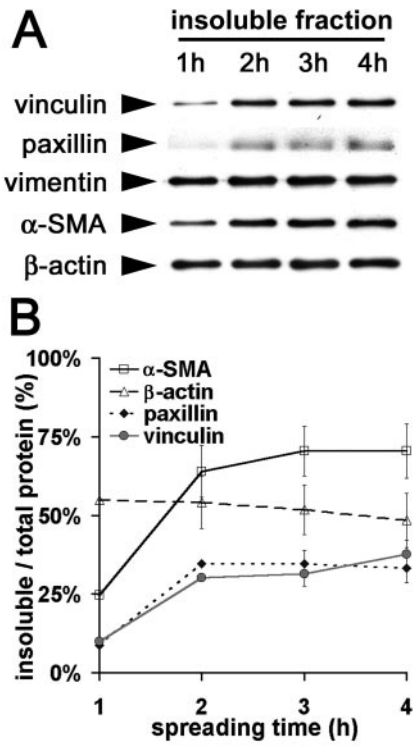

Figure 2. FA proteins and α-SMA codistribute in the TX-100–insoluble cytoskeletal fraction of spreading myofibroblasts. (A) TX-100 cytoskeletons were prepared of REF-52 fibroblasts after 1–4 h plating and investigated by means of Western blot. (B) Protein content in both, TX-100–soluble and –insoluble fractions were quantified by densitometry and the ratio of TX-100–insoluble protein/total protein was averaged from three independent experiments. Increase of FA proteins in the TX-100–insoluble fraction correlates with the increase of insoluble α-SMA.

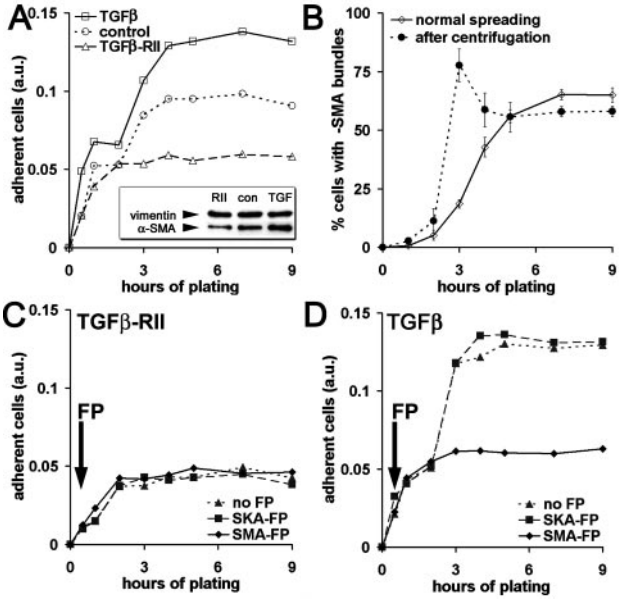

Figure 3. Appearance of α-SMA in filament bundles during spreading correlates with increased cell adhesion. (A) REF-52 with low (TGFβ-RII), medium (control), and high α-SMA expression (TGFβ) were plated for 0.5–9 h in serum-containing medium. Highly adhesive cells were selected by inverted centrifugation, stained with crystal violet, and quantified by photometry. After a first phase of low adhesion (phase 1), α-SMA–positive fibroblasts exhibit a second phase of strong adhesion (phase 2), which is absent in α-SMA–negative cells. (B) After plating, REF-52 were either centrifuged (♦) or directly fixed (◇) and stained for α-SMA and actin-phalloidin to determine the percentages of fibroblasts containing α-SMA filament bundles. After 3–4 h plating, centrifugation selects essentially cells with α-SMA filament bundles. (C and D) REF-52 were plated in serum-free conditions, optionally treated with FPs after 30 min (arrows), and centrifuged and adhesion was evaluated by crystal violet. SMA-FP has no effect on α-SMA–negative REF-52 (C), but inhibits phase 2 of α-SMA–positive fibroblast populations (D); the SKA-FP has no effect. One representative result out of five independent experiments is shown in A, C, and D; mean values from three independent experiments ±SD are presented in B.

The Level of α-SMA Expression in Long-period Culture Correlates with the Degree of FA Supermaturation and Fibroblast Adhesion

To test the relation between α-SMA expression, FA maturation and cell adhesion strength in well-developed fibroblasts with established FAs and stress fibers, we plated REF-52 for 5 d under different serum conditions (Figure 4, A–C). Under 20% FCS, cells exhibited only thin stress fibers that were negative for α-SMA, similar to cells treated with TGFβ-RII in 2% FCS (Figure 4A). Under 10% FCS, larger stress fibers coexpressed significant levels of α-SMA together with β-cytoplasmic actin (Figure 4B). The thickness of stress fibers and their content of α-SMA were further enhanced by lowering FCS concentration to 2%; this effect was similar to TGFβ treatment in 10% FCS (Figure 4C). Densitometry of Western blots demonstrated a significant increase of α-SMA with decreasing FCS concentration (Figure 4E) of maximum ~2.5-fold between culture in 20% FCS and 2% FCS. Vimentin and β-cytoplasmic actin expression did not change with different serum levels. Under these conditions we studied whether FA composition and morphology was affected. REF-52 grown in 2% FCS exhibited ~1.5-fold higher levels of vinculin, β3 integrin, and paxillin compared with the respective protein expression in 20% FCS. Interestingly, expression of α5β1 integrin decreased to 0.5-fold. In 20% FCS, α-SMA–negative REF-52 exhibited small FAs (2.3 ± 0.3 μm^2) that were restricted to the end of stress fibers, as revealed by immunostaining for vinculin (Figure 4A). In 10% FCS, FAs at the ends of α-SMA-containing stress fibers were larger (3.1 ± 0.5 μm^2, Figure 4B) and enlarged further in 2% FCS to 9.2 ± 0.5 μm^2; in this condition vinculin localized all along stress fibers (Figure 4C). Supermature FAs were already formed in 10% FCS and were identified by the colocalization of tensin and β3 integrin (Figure 4D); classical FAs of α-SMA–negative cells (20% FCS and TGFβ-RII) were devoid of tensin (our unpublished results). Supermature FAs contained no α5β1 integrin and thereby differed from tensin- and α5β1 integrin-containing fibrillar adhesions (Figure 4D); α5β1 integrin did not associate with stress fibers but with thinner actin bundles (our unpublished results).

To examine whether changes in the expression of α-SMA and major FA components influence cell adhesion, REF-52

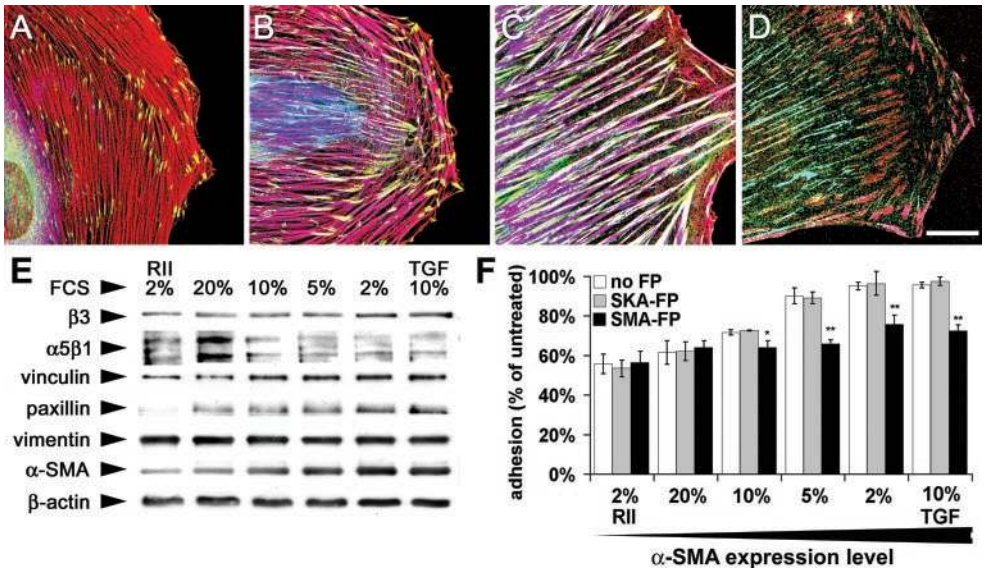

Figure 4. The adhesion capacity of fibroblasts in long-term culture correlates with their level of α-SMA expression and the degree of FA supermaturation. REF-52 were grown for 5 d in culture medium containing 20% FCS (A), 10% FCS (B and D), and 2% FCS (C). (A–C) Cells were immunostained for α-SMA (blue), vinculin (green), and β-cytoplasmic actin (red) and observed by confocal microscopy; shift from red to purple indicates increase in α-SMA expression. (D) Cells were stained for α5β1 integrin (green), tensin (blue), and β3 integrin (red); tensin colocalizes with β3 integrin in supermature FAs (pink) and with α5β1 integrin in fibrillar adhesions (turquoise). Bar, 25 μm. (E) REF-52 were plated for 5 d in different serum conditions, and protein expression was assessed by Western blotting. The expression levels of α-SMA, paxillin, vinculin, and β3 integrin increase with decreasing serum concentration. To test their adhesion capacity, REF-52 with different levels of α-SMA expression were trypsinized and plated for 2 d. After treatment with FPs and 0.02% EDTA for 60 min, weakly adherent cells were removed by centrifugation. Cell adhesion increases with increasing α-SMA expression. SMA-FP reduces the adhesion of α-SMA-expressing fibroblasts to the level of α-SMA–negative fibroblasts; SKA-FP has no effect.

grown for 5 d in different serum conditions were trypsinized and plated for 2 d. Similar to adhesion tests performed on spreading cells, REF-52 plated for longer time periods were inversely centrifuged. Fibroblast adhesion generally increased with decreasing serum levels (Figure 4), showing high correlation with the expression levels of α-SMA (r^2 = 0.89), vinculin (r^2 = 0.75), paxillin (r^2 = 0.73) and β3 integrin (r^2 = 0.65) and no correlation with vimentin (r^2 = 0.38), β-cytoplasmic actin (r^2 = 0.01) and α5β1 integrin (r^2 = −0.05). These data suggest a close functional correlation between cell adhesion, α-SMA expression and the molecular composition of FAs.

Inhibition of α-SMA Function Affects Supermature FAs and Decreases Adhesion of Established Myofibroblasts

To further investigate whether the high adhesion achieved in low serum conditions is related to α-SMA function, we treated the different populations with SMA-FP. The SMA-FP did not affect adhesion of α-SMA–negative fibroblasts and decreased myofibroblast adhesion in all conditions to the level of α-SMA–negative cells (Figure 4F). The SKA-FP was always without effect. To examine the effect of SMA-FP on FAs by videomicroscopy, we have transfected REF-52 with EGFP-constructs of β3 integrin (Figure 5A), paxillin (Figure 5B), and α5 integrin (Figure 5C). Transfection of the different components did not change the level of α-SMA expression; moreover, all constructs colocalized with the endogenous protein (our unpublished results). In control conditions, β3 integrin- and paxillin-EGFP–containing FAs exhibited extremely low dynamics. After addition of SMA-FP they started to slide centripetally and to disperse within 30 min (Figure 5, A and B). Concomitantly with its decrease in FAs, paxillin but not β3 integrin redistributed to fibrillar adhesion sites at the cell center (Figure 5B, arrowheads). Starting from 90 min after SMA-FP addition, FAs disappeared and cells retracted their lamellae. Interestingly, SMA-FP did not change the localization of α5 integrin in fibrillar adhesions (Figure 5C). The SKA-FP was always without effect.

To quantify the effect of SMA-FP on the distribution of β3 integrin-, paxillin-, and α5 integrin-EGFP, we evaluated the fluorescence intensity of these constructs in adhesion sites as a measure for their density (Figure 6A). FAs of untreated myofibroblasts (−30–0 min) and of cells treated with the SKA-FP (control, only shown for β3 integrin) maintained constant intensity levels of all tested EGFP-constructs. In FAs of cells treated with the SMA-FP paxillin-EGFP fluorescence decreased after 30 min to 70% of its initial intensity. This was followed by a significant decrease in β3 integrin-EGFP intensity (88% after 40 min); α5 integrin-EGFP intensity remained unaffected. Interestingly, paxillin-EGFP fluorescence increased in fibrillar adhesions ~50 min after SMA-FP treatment. In control cells, these central adhesion sites were negative for vinculin and β3 integrin (our unpublished results) and strongly positive for tensin and exhibited traces of paxillin (Figure 6B). Within 90 min of SMA-FP application, paxillin was enriched significantly (Figure 6C). In parallel, cells formed new lamellipodia that exhibited a seam of nascent focal complexes that were positive for paxillin (Figure 6C, arrowhead), vinculin, and β3 integrin (our unpublished results). When cells were immunostained after long-term treatment (5 d) with SMA-FP (3 μg/ml), tensin and α5β1 integrin were exclusively localized in fibrillar adhesions, whereas paxillin and β3 integrin were only present in classical FAs; supermature FAs were completely lost (our

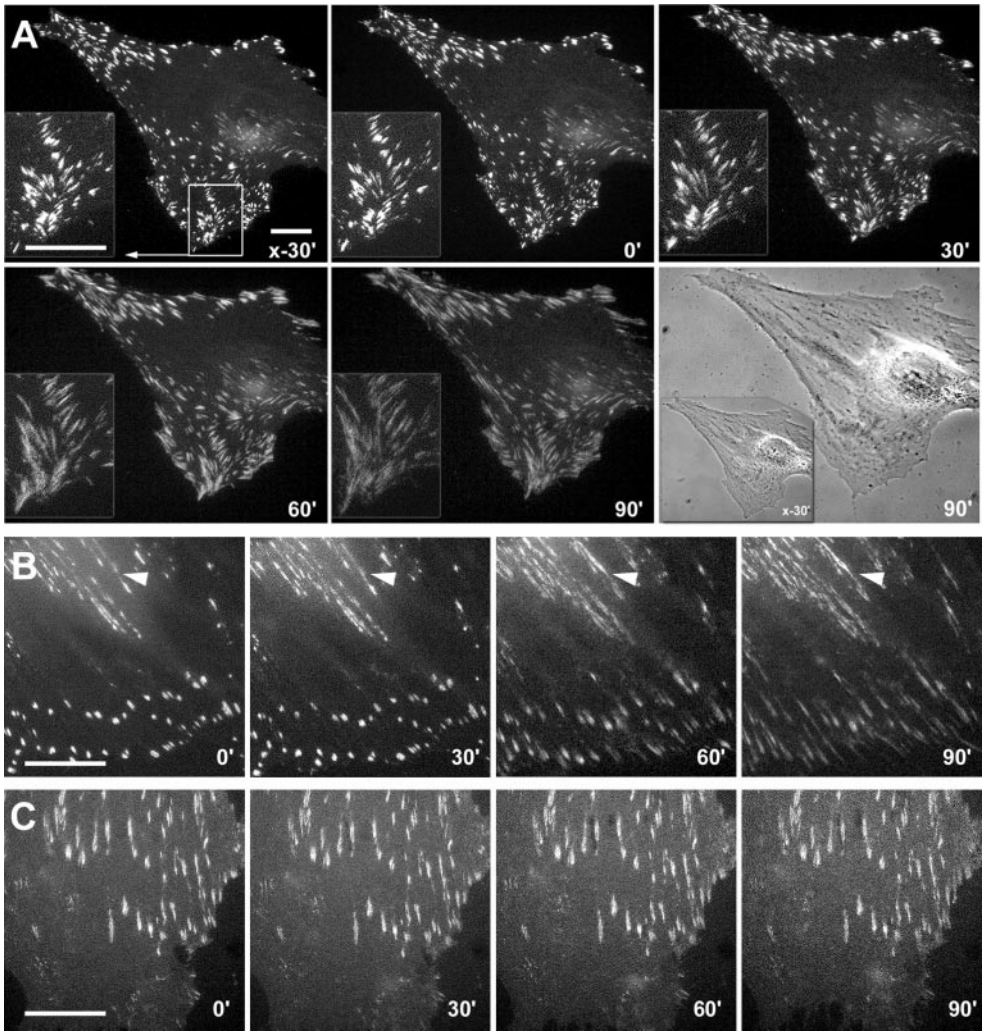

Figure 5. Application of the SMA-FP leads to dissociation of FAs. REF-52 myofibroblasts, transfected with EGFP-constructs of β3 integrin (A), paxillin (B), and α5 integrin (C) were treated with SMA-FP and observed by videomicroscopy; times of recording are indicated in the lower right corner. Application of SMA-FP leads to centripetal sliding and disassembly of β3 integrin- and paxillin-containing FAs. However, fibrillar adhesions that exhibit traces of paxillin (B, arrowheads) and strong expression of α5 integrin (C) remain stable. Bar, 20 μm.

unpublished results). The dispersion of FA components 90 min after SMA-FP treatment was accompanied by their increase in the TX-100–soluble fraction on the expense of a decrease in the TX-100–insoluble cytoskeletal fraction (Figure 6D); α-SMA exhibited only a minor shift to the soluble fraction, whereas $\alpha5\beta1$ integrin and vimentin did not change compared with control. These data suggest that α-SMA plays a crucial role in immobilizing the structural components of supermature FAs.

To test this hypothesis, we examined the turnover of β3 integrin in FAs by measuring FRAP of β3 integrin-EGFP. β3 integrin-EGFP in high α-SMA–expressing fibroblasts (TGFβ, our unpublished results) exhibited a half-maximal time of FRAP of ~18 min, compared with ~10 min in control cells, expressing medium levels of α-SMA (Figure 7). In these cells, the half-maximal FRAP time was significantly decreased to 5 min by the SMA-FP. These results suggest that α-SMA plays an important role in decreasing the turnover of proteins in supermature FAs and may thereby contribute to establishing stable adhesion sites.

Decrease of Myofibroblast Contractile Activity after SMA-FP Application Precedes Disassembly of FAs

One major function of α-SMA is increasing the contractile activity of stress fibers (Hinz *et al.*, 2001a), which is specifically inhibited by the SMA-FP (Hinz *et al.*, 2002). It is conceivable that the high α-SMA–mediated intracellular tension is crucial to maintain supermature FAs. To simultaneously analyze myofibroblast contractile activity and FA dynamics, we have grown paxillin- and β3 integrin-EGFP–transfected REF-52 on deformable micropatterned polyacrylamide substrates. The percentage of fibroblasts exhibiting α-SMA and supermature FAs gradually decreased with decreasing stiffness of the polyacrylamide substrates after 5-d culture; α-SMA expression was completely lost below a Young's modulus of 12.9 N/m^2 (0.05% BIS). We used substrates with an elasticity of 18.8 N/m^2 (0.075% BIS), on which contractile force was visible as small distortions in the imprinted micropattern in close vicinity to FAs (Figure 8, A, D, and G) and was restricted to α-SMA–positive cells. Twenty minutes after SMA-FP application, myofibroblasts relaxed strongly,

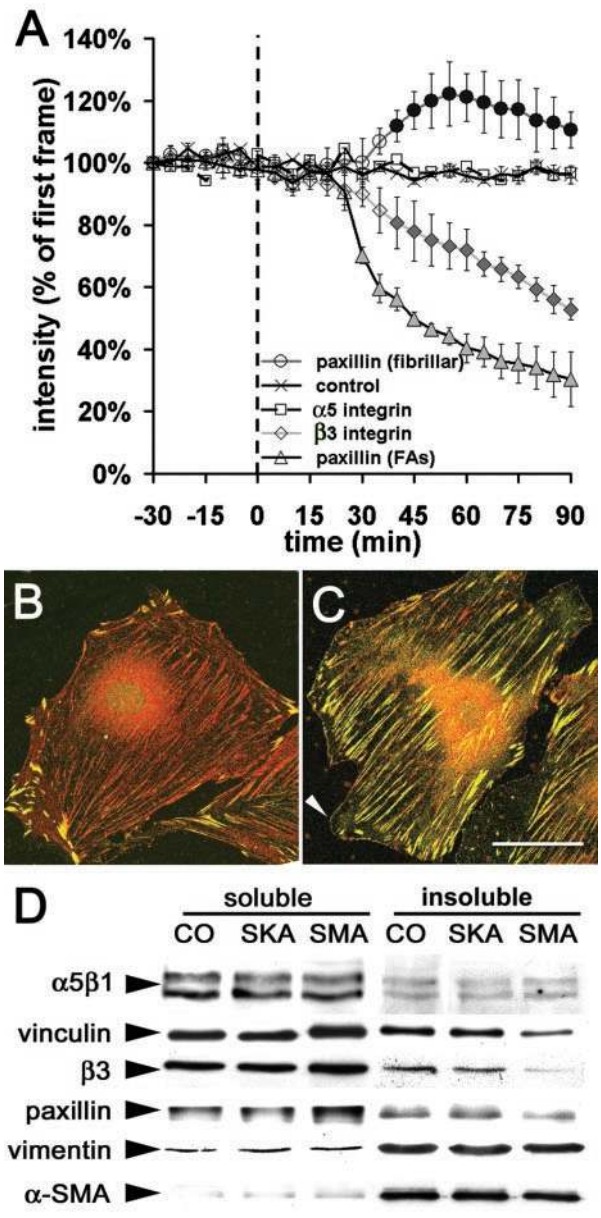

Figure 6. Application of SMA-FP leads to destabilization of FA components. (A) Sequences of fluorescence images were recorded from REF-52, transfected with β3 integrin-, paxillin-, and α5 integrin-EGFP. The fluorescence intensities of FAs and fibrillar adhesions were measured every 5 min, starting 30 min before and ending 90 min after application of SMA-FP and SKA-FP (control, shown for β3 integrin-EGFP). Each data point represents the average of 5–10 cells and 20 FAs per cell ±SD; filled symbols indicate $p \leq 0.01$ compared with control. REF-52 were treated for 90 min with SKA-FP (B) or SMA-FP (C) and immunostained against paxillin (green) and tensin (red). Note the shift of paxillin from supermature FAs to fibrillar adhesions and de novo formation of focal complexes (arrowhead). Bar, 50 μm. (D) TX 100–insoluble cytoskeletons were prepared 90 min after SMA-FP application and processed for Western blotting. Compared with controls, treatment with SMA-FP leads to a decrease of FA proteins in the TX 100–insoluble cytoskeletal fraction; fibrillar adhesion protein α5β1 integrin was not affected.

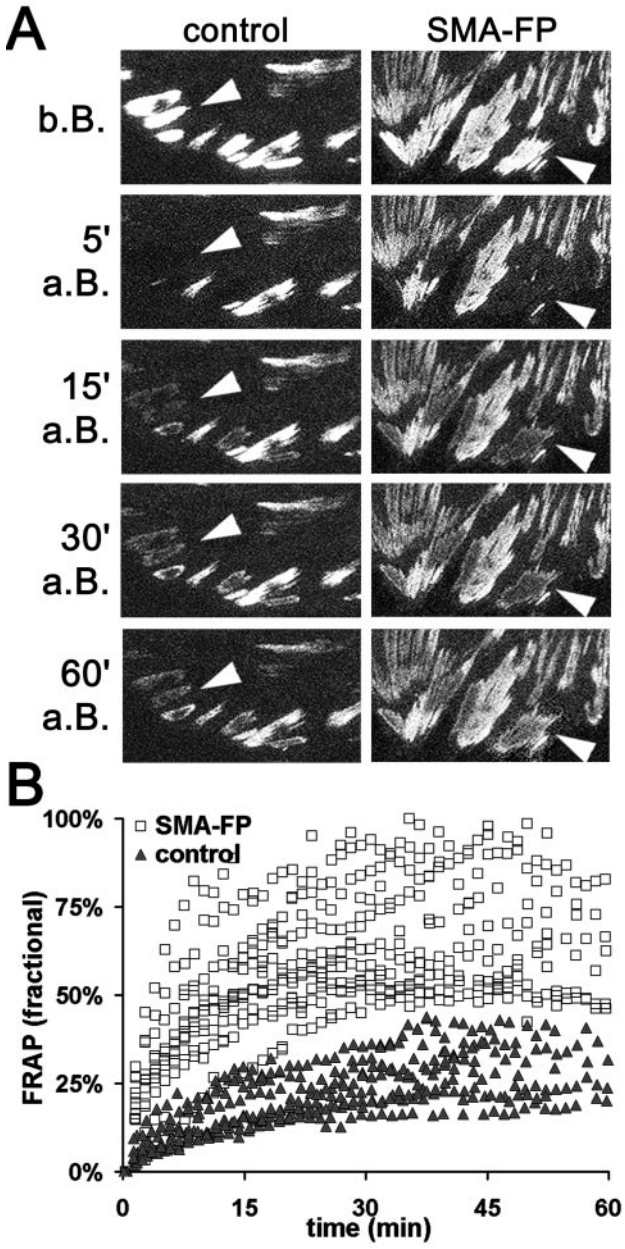

Figure 7. Turnover of β3 integrin increases in FAs after application of SMA-FP. (A) FAs of β3 integrin-EGFP-transfected REF-52 were photo-bleached (arrowheads) and FRAP in control conditions was compared with SMA-FP-treated cells (b.B., a.B.: before and after bleaching). Box width, 50 μm. (B) Fluorescence intensities were measured every minute and related to the intensity measured in the first video frame. Each data point represents the mean fractional FRAP of 12 FAs per cell; 12 cells were analyzed per condition. Note the increase in β3 integrin turnover after SMA-FP application.

leading to the restoration of a regular surface pattern (Figure 8B); at the time of relaxation paxillin density remained unchanged (Figure 8D). However, paxillin density decreased

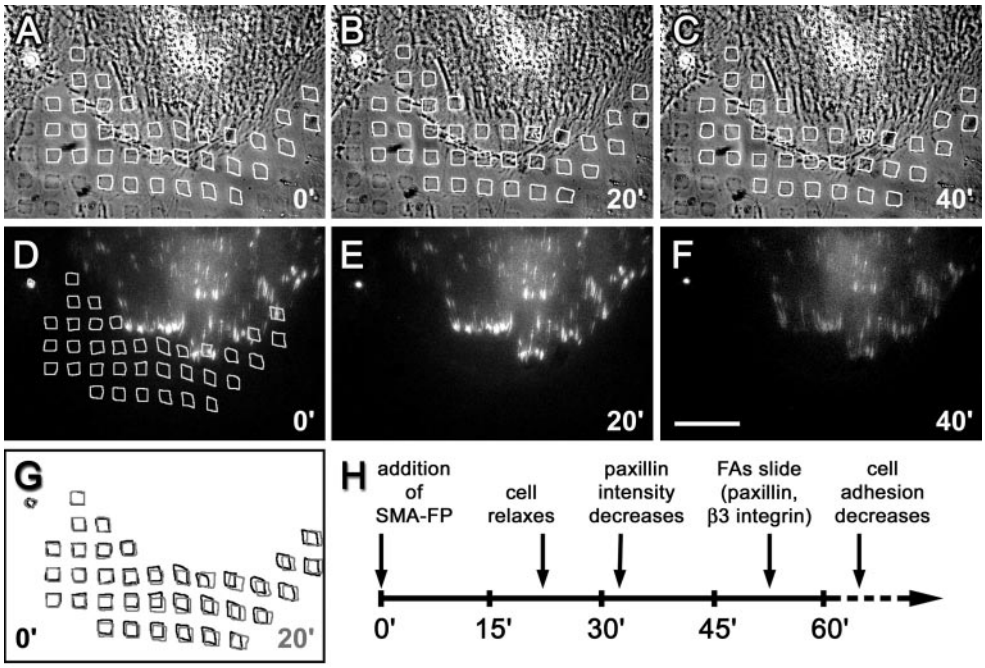

Figure 8. On SMA-FP application, myofibroblasts first loose contractile activity followed by FA destabilization. Paxillin-EGFP transfected REF-52 were grown on micropatterned flexible polyacrylamide substrates and observed by video microscopy. (A–C) Substrate deformation is visualized by distortions in the 5×5-μm pattern (highlighted by white squares) in phase contrast simultaneously to the observation of paxillin-EGFP–positive FAs in immunofluorescence (D–F). Video frames are shown immediately before (0 min, A and D), 20 min (B and E), and 40 min (C and F) after SMA-FP treatment. Bar, 50 μm. (G) Square pattern positions before (black) and 20 min after SMA-FP (gray) are superposed to highlight cell relaxation. The time course of cell relaxation and FA changes is schematized in H.

~5 min after cell relaxation (Figure 8F), followed by a decrease in β3 integrin density after another 5 min (our unpublished results). When FAs started to slide 30 min after the initial cell relaxation, the regular surface pattern was completely restored. This sequence of events (Figure 8G) suggests that the high contractile activity exerted by α-SMA is crucial to maintain supermature FAs.

DISCUSSION

Cultured myofibroblasts are characterized by the expression of α-SMA in stress fibers and the formation of specialized adhesion structures, recently termed supermature FAs (Dugina *et al.*, 2001; Tomasek *et al.*, 2002). The main objective of this study was to investigate the role of α-SMA in the maturation of FAs and in regulating the adhesion strength of myofibroblasts. We show that incorporation of α-SMA into stress fibers accelerates FA maturation during spreading and, in later culture periods stabilizes FAs, possibly by keeping a high intracellular contractile activity and by decreasing FA protein turnover. The overall result is increased adhesion strength. Such an effect may have important implications during wound healing, where dermal fibroblasts first migrate into the provisional clot matrix and start granulation tissue formation (for a review see Martin, 1997). This includes increased secretion of structural ECM proteins such as collagen and de novo expression of the FN splice variant ED-A FN (Serini *et al.*, 1998). Subsequently, they acquire a contractile phenotype (Welch *et al.*, 1990; Hinz *et al.*, 2001b), i.e., express α-SMA (Darby *et al.*, 1990) and form a specialized adhesion complex, called fibronexus (Singer, 1979).

The fibronexus is characterized by a firm coalignment of intracellular actin fibers with extracellular FN fibrils, which in turn are connected to collagen in the wound matrix (Singer *et al.*, 1984). We have recently proposed supermature FAs of cultured myofibroblasts as a suitable in vitro model for the fibronexus (Dugina *et al.*, 2001). In contrast to classical FAs, they exhibit a tight association with FN and contain significant levels of tensin but clearly differ from FN-associated, tensin–positive fibrillar adhesions by expressing high levels of vinculin, paxillin, and β3 integrin. In REF-52, supermature FAs are distinguishable from fibrillar adhesion by the absence of $\alpha 5\beta 1$ integrin; this is in contrast to supermature FAs of TGF-β-treated human subcutaneous and Dupuytren's fibroblasts (Dugina *et al.*, 2001), which express similar levels of α-SMA and may be due to the recruitment different FN receptors, specific for ED-A FN (Liao *et al.*, 2002). The physiological significance of supermature FAs is further supported by a recent study on "3D matrix adhesions" of fibroblasts cultured on mouse embryo tissue sections (Cukierman *et al.*, 2001). Similar to supermature FAs, these 3D matrix adhesions exhibit an overlapping pattern of typical fibrillar and classical FA marker proteins, remarkably a colocalization of paxillin and vinculin with tensin and fibronectin fibrils. Interestingly, embryonic mesenchyme resembles wound granulation tissue by containing high levels of ED-A FN (Ffrench-Constant *et al.*, 1989); further studies using wound granulation tissue sections as 3D substrates will provide further insight into the molecular composition of the fibronexus. Formation of the fibronexus intensifies myofibroblast adhesion with the wound matrix (Singer *et al.*, 1984). Increased adhesion may serve a) to immobilize cells in the wound bed and b) to permit an efficient transduction of intracellular contractile force to the substrate in order to reorganize the matrix and to contract the wound (for a review see Tomasek *et al.*, 2002).

The strength of fibroblast adhesion correlated with the level of α-SMA expression in all situations studied. By using 5-d fibroblast culture in low serum we could induce an important α-SMA expression and stress fiber formation,

thereby differing from classical technique of serum-starving for 2–24 h that reduces fibroblast stress fiber formation. Expression of α-SMA increases fibroblast adhesion presumably by promoting supermaturation of FAs. The increased size of supermature FAs alone may be sufficient to promote high adhesion, because FA force transmission has recently been shown to be linearly proportional to their size (Balaban *et al.,* 2001). Intracellular and extracellular stress have been shown to be major inducers for the maturation of small focal complexes into classical FAs and their further enlargement (for a review see Geiger and Bershadsky, 2001). Increasing intracellular contractile activity by activating the Rho-kinase pathway was shown to increase FA size (Ridley and Hall, 1992; Ballestrem *et al.,* 2001). Conversely, a wide range of inhibitors of actomyosin contractile activity act to disassemble FAs or keep them in their immature state as small focal complexes (Volberg *et al.,* 1994; Chrzanowska Wodnicka and Burridge, 1996; Helfman *et al.,* 1999; Kaverina *et al.,* 1999). Extracellular stress reinforces contact formation, when matrix-coated beads are restrained on the dorsal surface of cultured cells (Choquet *et al.,* 1997; Suter *et al.,* 1998) and can even bypass the need for intracellular contractile activity when cell edges are pulled with the use of microneedles (Riveline *et al.,* 2001). Relaxing prestretched silicone substrates reduces fibroblast FA size (Sawada and Sheetz, 2002) and growing cells on compliant polyacrylamide substrates inhibits FA maturation (Pelham and Wang, 1997).

Similarly, the further differentiation of classical FAs into supermature FAs requires mechanical tension; it was here prevented by growing myofibroblasts on compliant substrates and was inhibited by the use of general inhibitors of actomyosin contraction (Dugina *et al.,* 2001). Several results support the suggestion that the high tension needed for supermature FA formation in myofibroblasts is created by α-SMA, which mediates a higher contractile activity compared with α-SMA–negative fibroblasts (Arora and McCulloch, 1994; Hinz *et al.,* 2001a, 2001b).

1. The specific inhibition of α-SMA–mediated contractile activity of myofibroblasts by SMA-FP (Hinz *et al.,* 2002) precedes the dispersion of FAs, as demonstrated with the use of micropatterned flexible polyacrylamide substrates. The subsequent accumulation of tension-independent focal complexes at lamellar tips further indicates the loss of mechanical stress. It is not clear why supermature FAs are first completely disassembled and do not directly convert into later reformed classical FAs, because myofibroblasts keep a low contractile activity after application of SMA-FP (Hinz *et al.,* 2002). One possibility is the effect of the AcEEED peptide on α-SMA polymerization (Chaponnier *et al.,* 1995); thus, SMA-FP may influence the distribution of FA proteins that are physically linked to α-SMA independent of its NH_2-terminus.

2. The fluorescence intensity of β3 integrin- and paxillin-EGFP in supermature FAs decreased upon treatment with the SMA-FP, similar to that of vinculin-EGFP after actomyosin inhibition by BDM (Balaban *et al.,* 2001) and to that of β3 integrin-EGFP after Rho-kinase inhibition by Y27632 (Ballestrem *et al.,* 2001). Conversely, induction of cell contractility by LPA or by transfection of dominant active RhoA was demonstrated to increase β3 integrin density in FAs. When assessed by FRAP analysis, β3 integrin turnover was shown to be low in stable and high in sliding FAs (Ballestrem *et al.,* 2001). Thus, the faster FRAP of supermature FAs after SMA-FP indicates a decrease in FA stability.

3. The SMA-FP had no effect on fibrillar adhesions that are not affected by inhibition of actomyosin contractile activity (Katz *et al.,* 2000). Interestingly, we observed an exchange of paxillin from FAs to fibrillar adhesions after myofibroblast relaxation by SMA-FP. Paxillin was the earliest FA protein reacting to the loss of α-SMA–mediated tension as summarized in Figure 8G. It was recently shown to increase in mechanically pulled adhesion sites in contrast to other FA proteins such as vinculin (Riveline *et al.,* 2001) and to specifically accumulate in stretched TX-100 cytoskeletons (Sawada and Sheetz, 2002). Further studies are needed to clarify whether paxillin may play a key role in transmitting biomechanical signals in addition to its suggested role as an important mediator of growth factor-related signals (Turner, 2000).

4. During spreading, maturation of FAs and increase of myofibroblast adhesion correlated with the incorporation of α-SMA into stress fibers and were inhibited by the SMA-FP. The first cortical filament bundles of spreading myofibroblasts contained exclusively β-cytoplasmic actin, which was followed by α-SMA incorporation into stress fibers ~60 min later. Actin isoforms differ essentially in their N-terminus (Vandekerckhove and Weber, 1978), rendering this domain as a favorable candidate for intracellular targeting. We have shown recently that the SMA-FP localizes to stress fibers of myofibroblasts (Hinz *et al.,* 2002), suggesting the presence of a specific AcEEED-recognition site in these structures. Hence, the availability of such a site may be the limiting factor for the incorporation of α-SMA into existing β-cytoplasmic actin bundles. We suggest that myofibroblast adhesion sites are initially organized by β-cytoplasmic actin bundles and subsequently reinforced by α-SMA–mediated contractile activity; this is in agreement with the close correlation between the cytoskeletal stabilization of α-SMA and FA proteins paxillin and vinculin.

We conclude that expression of α-SMA increases the mechanical strength of FAs by increasing stress fiber contractile activity. The resulting enlargement and supermaturation of FAs allows more efficient force transmission, thereby augmenting tension in the ECM. In turn, increased matrix tension increases α-SMA expression as shown for fibroblasts in attached collagen gels (Arora *et al.,* 1999) and in mechanically stressed wounds (Hinz *et al.,* 2001b). Understanding the molecular key players in this mechanical feedback loop may help to prevent situations where its dysregulation turns into a vicious cycle, such as in the formation of hypertrophic scars and in a variety of fibro-contractive diseases.

ACKNOWLEDGMENTS

We gratefully thank Dr. G. Gabbiani for his invaluable and constant scientific help and for providing his laboratory facilities. We thank G. Celetta, J. Lussi, P. Louzao, M. Bacchetta, A. Maurer-Hiltbrunner, M.C. Jacquier, J.C. Rumbeli and Dr. Sophie Clément for expert help in the different techniques and Dr. Alexander Verkhovsky for critical reading of the manuscript. Drs. B. Geiger and A. Bershadsky, A.F. Horwitz, J.A. Hubbell, V. Koteliansky, and V. Belkin are gratefully acknowledged for providing paxillin-EGFP, α5 integrin-EGFP, TGFβ-RII, patterned Si wafers, and α5β1 integrin antibody, respectively. This work was supported by the Swiss National Science Foundation (Grants 31-61336.00, 31-68313.02, and 31-54048.98) and UCB Bioproducts.

REFERENCES

Adams, J.C. (2001). Cell-matrix contact structures. Cell Mol. Life Sci. *58,* 371–392.

Arora, P.D., and McCulloch, C.A. (1994). Dependence of collagen remodelling on alpha-smooth muscle actin expression by fibroblasts. J. Cell. Physiol. *159,* 161–175.

Arora, P.D., Narani, N., and McCulloch, C.A. (1999). The compliance of collagen gels regulates transforming growth factor-beta induction of alpha-smooth muscle actin in fibroblasts. Am. J. Pathol. *154,* 871–882.

Balaban, N.Q. *et al.* (2001). Force and focal adhesion assembly: a close relationship studied using elastic micropatterned substrates. Nat. Cell Biol. *3,* 466–472.

Ballestrem, C., Hinz, B., Imhof, B.A., and Wehrle-Haller, B. (2001). Marching at the front and dragging behind: differential alphaVbeta3-integrin turnover regulates focal adhesion behavior. J. Cell Biol. *155,* 1319–1332.

Calderwood, D.A., Shattil, S.J., and Ginsberg, M.H. (2000). Integrins and actin filaments: reciprocal regulation of cell adhesion and signaling. J. Biol. Chem. *275,* 22607–22610.

Chaponnier, C., Goethals, M., Janmey, P.A., Gabbiani, F., Gabbiani, G., and Vandekerckhove, J. (1995). The specific NH2-terminal sequence Ac-EEED of alpha-smooth muscle actin plays a role in polymerization in vitro and in vivo. J. Cell Biol. *130,* 887–895.

Choquet, D., Felsenfeld, D.P., and Sheetz, M.P. (1997). Extracellular matrix rigidity causes strengthening of integrin-cytoskeleton linkages. Cell *88,* 39–48.

Chrzanowska Wodnicka, M., and Burridge, K. (1996). Rho-stimulated contractility drives the formation of stress fibers and focal adhesions. J. Cell Biol. *133,* 1403–1415.

Clark, E.A., King, W.G., Brugge, J.S., Symons, M., and Hynes, R.O. (1998). Integrin-mediated signals regulated by members of the rho family of GTPases. J. Cell Biol. *142,* 573–586.

Cukierman, E., Pankov, R., Stevens, D.R., and Yamada, K.M. (2001). Taking cell-matrix adhesions to the third dimension. Science *294,* 1708–1712.

Darby, I., Skalli, O., and Gabbiani, G. (1990). Alpha-smooth muscle actin is transiently expressed by myofibroblasts during experimental wound healing. Lab. Invest. *63,* 21–29.

Derossi, D., Joliot, A.H., Chassaing, G., and Prochiantz, A. (1994). The third helix of the Antennapedia homeodomain translocates through biological membranes. J. Biol. Chem. *269,* 10444–10450.

Desmoulière, A., Geinoz, A., Gabbiani, F., and Gabbiani, G. (1993). Transforming growth factor-beta 1 induces alpha-smooth muscle actin expression in granulation tissue myofibroblasts and in quiescent and growing cultured fibroblasts. J. Cell Biol. *122,* 103–111.

Dugina, V., Fontao, L., Chaponnier, C., Vasiliev, J., and Gabbiani, G. (2001). Focal adhesion features during myofibroblastic differentiation are controlled by intracellular and extracellular factors. J. Cell Sci. *114,* 3285–3296.

Ffrench-Constant, C., Van de Water, L., Dvorak, H.F., and Hynes, R.O. (1989). Reappearance of an embryonic pattern of fibronectin splicing during wound healing in the adult rat. J. Cell Biol. *109,* 903–914.

Gabbiani, G., Ryan, G.B., and Majno, G. (1971). Presence of modified fibroblasts in granulation tissue and their possible role in wound contraction. Experientia *27,* 549–550.

Geiger, B., and Bershadsky, A. (2001). Assembly and mechanosensory function of focal contacts. Curr. Opin. Cell Biol. *13,* 584–592.

Geiger, B., Bershadsky, A., Pankov, R., and Yamada, K.M. (2001). Transmembrane crosstalk between the extracellular matrix and the cytoskeleton. Nat. Rev. Mol. Cell. Biol. *2,* 793–805.

Helfman, D.M., Levy, E.T., Berthier, C., Shtutman, M., Riveline, D., Grosheva, I., Lachish-Zalait, A., Elbaum, M., and Bershadsky, A.D. (1999). Caldesmon inhibits nonmuscle cell contractility and interferes with the formation of focal adhesions. Mol. Biol. Cell *10,* 3097–3112.

Hinz, B., Celetta, G., Tomasek, J.J., Gabbiani, G., and Chaponnier, C. (2001a). Alpha-smooth muscle actin expression upregulates fibroblast contractile activity. Mol. Biol. Cell *12,* 2730–2741.

Hinz, B., Gabbiani, G., and Chaponnier, C. (2002). The NH2-terminal peptide of alpha-smooth muscle actin inhibits force generation by the myofibroblast in vitro and in vivo. J. Cell Biol. *157,* 657–663.

Hinz, B., Mastrangelo, D., Iselin, C.E., Chaponnier, C., and Gabbiani, G. (2001b). Mechanical tension controls granulation tissue contractile activity and myofibroblast differentiation. Am. J. Pathol. *159,* 1009–1020.

Hynes, R.O. (1999). Cell adhesion: old and new questions. Trends Cell Biol. *9,* M33–37.

Katz, B.Z., Zamir, E., Bershadsky, A., Kam, Z., Yamada, K.M., and Geiger, B. (2000). Physical state of the extracellular matrix regulates the structure and molecular composition of cell-matrix adhesions. Mol. Biol. Cell *11,* 1047–1060.

Kaverina, I., Krylyshkina, O., and Small, J.V. (1999). Microtubule targeting of substrate contacts promotes their relaxation and dissociation. J. Cell Biol. *146,* 1033–1044.

Komesli, S., Vivien, D., and Dutartre, P. (1998). Chimeric extracellular domain type II transforming growth factor (TGF)-beta receptor fused to the Fc region of human immunoglobulin as a TGF- beta antagonist. Eur. J. Biochem. *254,* 505–513.

Laukaitis, C.M., Webb, D.J., Donais, K., and Horwitz, A.F. (2001). Differential dynamics of alpha 5 integrin, paxillin, and alpha-actinin during formation and disassembly of adhesions in migrating cells. J. Cell Biol. *153,* 1427–1440.

Liao, Y.F., Gotwals, P.J., Koteliansky, V.E., Sheppard, D., and Van De Water, L. (2002). The EIIIA segment of fibronectin is a ligand for integrins alpha 9beta 1 and alpha 4beta 1 providing a novel mechanism for regulating cell adhesion by alternative splicing. J. Biol. Chem. *277,* 14467–14474.

Martin, P. (1997). Wound healing—aiming for perfect skin regeneration. Science *276,* 75–81.

Michel, R., Lussi, J.W., Csucs, G., Reviakine, I., Danuser, G., Ketterer, B., Hubbell, J.A., Textor, M., and Spencer, N.D. (2002). Selective molecular assembly patterning: a new approach to micro- and nanochemical patterning of surfaces for biological applications. Langmuir *18,* 3281–3287.

Nobes, C.D., and Hall, A. (1995). Rho, rac, and cdc42 GTPases regulate the assembly of multimolecular focal complexes associated with actin stress fibers, lamellipodia and filopodia. Cell *81,* 53–62.

Pelham, R.J., Jr., and Wang, Y. (1997). Cell locomotion and focal adhesions are regulated by substrate flexibility. Proc. Natl. Acad. Sci. USA *94,* 13661–13665.

Ridley, A.J., and Hall, A. (1992). The small GTP-binding protein rho regulates the assembly of focal adhesions and actin stress fibers in response to growth factors. Cell *70,* 389–399.

Riveline, D., Zamir, E., Balaban, N.Q., Schwarz, U.S., Ishizaki, T., Narumiya, S., Kam, Z., Geiger, B., and Bershadsky, A.D. (2001). Focal contacts as mechanosensors: externally applied local mechanical force induces growth of focal contacts by an mDia1-dependent and ROCK-independent mechanism. J. Cell Biol. *153,* 1175–1186.

Rønnov-Jessen, L., and Petersen, O.W. (1996). A function for filamentous alpha-smooth muscle actin: retardation of motility in fibroblasts. J. Cell Biol. *134,* 67–80.

Rønnov-Jessen, L., and Petersen, O.W. (1993). Induction of alpha-smooth muscle actin by transforming growth factor-beta 1 in quiescent human breast gland fibroblasts. Implications for myofibroblast generation in breast neoplasia. Lab. Invest. *68,* 696–707.

Rottner, K., Hall, A., and Small, J.V. (1999). Interplay between Rac and Rho in the control of substrate contact dynamics. Curr. Biol. *9,* 640–648.

Sawada, Y., and Sheetz, M.P. (2002). Force transduction by Triton cytoskeletons. J. Cell Biol. *156,* 609–615.

Serini, G., Bochaton-Piallat, M.L., Ropraz, P., Geinoz, A., Borsi, L., Zardi, L., and Gabbiani, G. (1998). The fibronectin domain ED-A is crucial for myofibroblastic phenotype induction by transforming growth factor-beta1. J. Cell Biol. *142,* 873–881.

Serini, G., and Gabbiani, G. (1999). Mechanisms of myofibroblast activity and phenotypic modulation. Exp. Cell Res. *250,* 273–283.

Singer, I.I. (1979). The fibronexus: a transmembrane association of fibronectin-containing fibers and bundles of 5 nm microfilaments in hamster and human fibroblasts. Cell *16,* 675–685.

Singer, I.I., Kawka, D.W., Kazazis, D.M., and Clark, R.A. (1984). In vivo co-distribution of fibronectin and actin fibers in granulation tissue: immunofluorescence and electron microscope studies of the fibronexus at the myofibroblast surface. J. Cell Biol. *98,* 2091–2106.

Skalli, O., Ropraz, P., Trzeciak, A., Benzonana, G., Gillessen, D., and Gabbiani, G. (1986). A monoclonal antibody against alpha-smooth muscle actin: a new probe for smooth muscle differentiation. J. Cell Biol. *103,* 2787–2796.

Suter, D.M., Errante, L.M., Belotserkovsky, V., and Forscher, P. (1998). The Ig superfamily cell adhesion molecule, ApCAM, mediates growth cone steering by substrate-cytoskeletal coupling. J. Cell Biol. *141,* 227–240.

Tomasek, J.J., Gabbiani, G., Hinz, B., Chaponnier, C., and Brown, R.A. (2002). Myofibroblasts and mechano-regulation of connective tissue remodelling. Nat. Rev. Mol. Cell. Biol. *3,* 349–363.

Turner, C.E. (2000). Paxillin and focal adhesion signalling. Nat. Cell Biol. *2,* E231–236.

Vandekerckhove, J., and Weber, K. (1978). At least six different actins are expressed in a higher mammal: an analysis based on the amino acid sequence of the amino-terminal tryptic peptide. J. Mol. Biol. *126,* 783–802.

Volberg, T., Geiger, B., Citi, S., and Bershadsky, A.D. (1994). Effect of protein kinase inhibitor H-7 on the contractility, integrity, and membrane anchorage of the microfilament system. Cell Motil. Cytoskel. *29,* 321–338.

Welch, M.P., Odland, G.F., and Clark, R.A. (1990). Temporal relationships of F-actin bundle formation, collagen and fibronectin matrix assembly, and fibronectin receptor expression to wound contraction. J. Cell Biol. *110,* 133–145.

Wilkins, J.A., Stupack, D., Stewart, S., and Caixia, S. (1991). Beta 1 integrin-mediated lymphocyte adherence to extracellular matrix is enhanced by phorbol ester treatment. Eur. J. Immunol. *21,* 517–522.

Yao, X., Chaponnier, C., Gabbiani, G., and Forte, J.G. (1995). Polarized distribution of actin isoforms in gastric parietal cells. Mol. Biol. Cell *6,* 541–557.

Zamir, E., Katz, B.Z., Aota, S., Yamada, K.M., Geiger, B., and Kam, Z. (1999). Molecular diversity of cell-matrix adhesions. J. Cell Sci. *112* (Pt 11), 1655–1669.

Zamir, E. *et al.* (2000). Dynamics and segregation of cell-matrix adhesions in cultured fibroblasts. Nat. Cell Biol. *2,* 191–196.